Phase Stabilization of a Frequency Comb using Multipulse Quantum Interferometry

Andrea Cadarso,[1,2] Jordi Mur-Petit,[1,3] and Juan José García-Ripoll[1]
[1]*Instituto de Física Fundamental, IFF-CSIC, Serrano 113 b, Madrid 28006, Spain*
[2]*Departamento de Análisis Matemático, Universidad Complutense de Madrid, 24040 Madrid, Spain*
[3]*Instituto de Estructura de la Materia, IEM-CSIC, Serrano 123, Madrid 28006, Spain*
(Received 7 March 2013; revised manuscript received 3 October 2013; published 21 February 2014)

From the interaction between a frequency comb and an atomic qubit, we derive quantum protocols for the determination of the carrier-envelope offset phase, using the qubit coherence as a reference, and without the need of frequency doubling or an octave spanning comb. Compared with a trivial interference protocol, the multipulse protocol results in a polynomial enhancement of the sensitivity $\mathcal{O}(N^{-2})$ with the number N of laser pulses involved. We specialize the protocols using optical or hyperfine qubits, Λ schemes, and Raman transitions, and introduce methods where the reference is another phase-stable cw laser or frequency comb.

DOI: 10.1103/PhysRevLett.112.073603 PACS numbers: 42.50.St, 03.67.Ac, 07.60.Ly, 42.62.Eh

Quantum physics has experienced a universally recognized [1] progress in the control and observation of individual quantum systems. In this respect, trapped ions [2,3] are one of the most mature setups, with unbeaten precision in the realization of single- [4] and two-qubit [5] unitaries and measurements [6,7], closely followed by neutral atoms [8]. This spectacular progress underlies a number of "spin offs," such as the characterization of atomic properties using entanglement [9] or the development of quantum algorithms and protocols [10–12] for studying molecular ions. The synergy is even more advanced in the field of metrology, with accurate atomic clocks assisted by quantum gates [13,14] or the use of atomic squeezing for enhanced magnetometry [15,16].

Despite the exquisite precision of atomic, molecular and optical (AMO) systems, the control and detection time scales ($\sim$10 μs to 10 ms) prevented using these techniques for studying ultrafast processes. In this work, we show that the speed of AMO setups is sufficient to accurately stabilize the carrier-envelope offset phase (CEP) of a frequency comb (FC). CEP effects are relevant for few-cycle pulses, though effects in multicycle pulses have also been reported [17]. The first observation of CEP effects was reported in the spatial asymmetry of above-threshold ionization from Kr gas [18] and in x-ray emission from Ne [19]. The direction of photocurrents injected in semiconductors is also controlled by the CEP [20,21] and the absolute CEP of single pulses was recently measured [22]. The study of the CEP has been generally centered on its spectral components [23], while only a few reports have addressed time-domain measurements of the relative phase of successive pulses in a train [24,25]. The methods presented below follow this less-beaten path.

Let us introduce the notion of "multipulse quantum interferometry" (MPQI), where an atom acts as a nonlinear, fast-response detector that efficiently measures the differences between ultrashort laser pulses. Modeling the atom-pulse interaction as a sequence of unitaries $\{U_i\}_{i=1}^N$ through a suitable reordering of the pulses, additional gates, and measurements, we build protocols that accurately determine the differences among the pulses, or the properties of individual pulses themselves. Compared with cw laser interferometry, this approach provides a polynomial enhancement of the sensitivity because a single atom accumulates many interferometric events.

A direct application of MPQI is the characterization and stabilization of a frequency comb [26,27]. This device produces a train of laser pulses with a fixed duration τ and a regular spacing T [cf. Fig. 1(a)]. Stabilizing a comb is ensuring that the offset frequency ν_0 remains a constant and well-known value, and that the spectrum is a collection of regularly spaced teeth with frequencies $f_n = n/T + \nu_0$ [Fig. 1(b)]. Haensch and Hall solved this problem [28,29] in frequency space, interferometrically comparing different teeth in the limit of many pulses. Note that this requires a comb whose spectrum spans at least an octave, or broadening the light with a nonlinear fiber. This stabilization enables direct frequency comb spectroscopy, accurately revealing the atomic level structure of neutral atoms [30,31] and ions [32,33].

We rather work on the time-domain image of the pulse train. The effect of the offset frequency is to change the CEP from pulse to pulse, $\phi_{n+1} - \phi_n = \Delta\phi = \nu_0 T$ [cf. Fig. 1(a)]. To address the problem of comb stabilization we will use MPQI, designing protocols that detect the phase difference between pulses with the greatest accuracy possible. We start by proposing a simple two-level protocol for consecutive pulses in a low intensity regime (1A) and in a $\theta \simeq \pi$ regime (1B). We further this study by introducing analogous protocols for delayed sequences of pulses, which display an enhanced sensitivity (protocols 2A and 2B). Afterwards, in order to minimize spontaneous emission, we

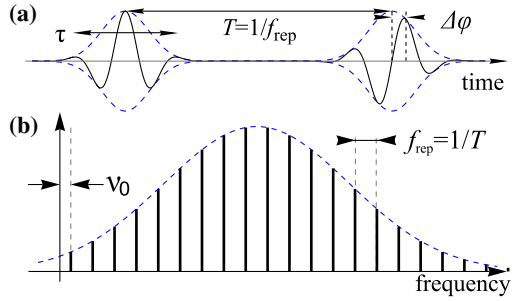

FIG. 1 (color online). (a) Electric field amplitude (solid line) and envelope (dashed) of a pulsed laser with period T and pulse-to-pulse phase difference $\Delta\phi$. (b) Associated spectra: a broad peak for one pulse (dashed) and a modulated comb for a pulse train with repetition rate f_{rep} (solid). The frequency offset ν_0 depends on the pulse-to-pulse phase difference $\Delta\phi$.

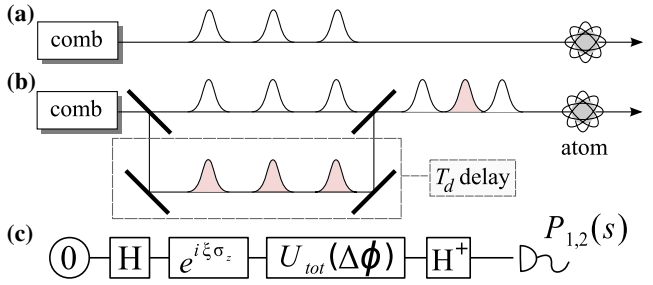

FIG. 2 (color online). Comb phase measurement setups. A trapped atom interacts with (a) one train of pulses or (b) two trains with a delay T_d. (c) Additional gates and a final state interrogation build up a generalized Ramsey interferometry protocol to estimate $\Delta\phi$ and θ.

describe equivalent protocols using Raman schemes. Finally, we present a discussion of experimental errors and the achievable sensitivities in practical implementations. The resulting methods do not require an octave-spanning comb, broadening, or frequency doubling. They are thus useful for a wider variety of lasers, demand less power, and may profit from the ever-growing precision in atomic interferometry.

Single-pulse unitary.—We start by determining the unitaries associated to each laser pulse and how they depend on the CEP ϕ_n. The interaction of multilevel atoms with a frequency comb was studied previously [34]. We model this interaction in the rotating wave approximation (RWA) in order to produce analytical results [35]

$$H_{\mathrm{RWA}} = \frac{1}{2}(\omega_{at} - \bar{\omega})\sigma_z + s(t)(e^{-i\phi_m}\sigma^+ + \mathrm{H.c.}), \quad (1)$$

Here, m is the pulse index, $s(t) \geq 0$is the pulse envelope, $\bar{\omega} = 2\pi\bar{\nu}$ is the comb carrier frequency, ω_{at} is the atomic transition frequency ($\hbar = 1$ throughout), there is an unknown phase ϕ_m for each pulse, and $\sigma_{x,y,z}$ are the Pauli matrices. The RWA works for pulses that contain ≥ 30 periods of the carrier frequency, $\tau \geq 30/\bar{\nu}$ (see the Supplemental Material [36]), and allows us to explicitly write the pulse unitaries

$$U_m = \cos\left(\frac{\theta_m}{2}\right) + i\sin\left(\frac{\theta_m}{2}\right)\sigma_{\phi_m} = e^{-i\phi_m\sigma_z}U_0 e^{i\phi_m\sigma_z} \quad (2)$$

in terms of the total Rabi flip angle of a single pulse, $\theta_m = 2\int_{-\tau/2}^{\tau/2} s(t)dt$, with $\sigma_{\phi_m} = \cos(\phi_m)\sigma_x + \sin(\phi_m)\sigma_y$. In what follows, we assume that the comb is almost resonant, $\bar{\omega} \simeq \omega_{at}$, and has uniform intensity, i.e., $\theta_m = \theta$. These assumptions imply that we only need to stabilize the pulse-to-pulse phase difference $\Delta\phi$.

Multipulse unitaries.—We want a protocol that efficiently detects the difference between a sequence of unequal pulses $U_{\mathrm{tot}} = \prod_{i=1}^{N} U_i$, and the ideal case U_1^N. Let us first assume an ideal qubit, seeking an ordering of pulses with which the fidelity $|\mathrm{tr}(U_1^{N\dagger}U_{\mathrm{tot}})|$ decreases most rapidly with N. The simplest protocol (1A) applies N consecutive pulses [cf. Fig. 2(a)] with low intensity, $\theta \ll 1$, on the qubit, which adiabatically follows the phase

$$U_{\mathrm{tot}}^{(1A)} \approx \mathbb{1} + i\theta\frac{\sin(N\Delta\phi)}{2\sin(\Delta\phi)}[e^{i(N+1)\Delta\phi}\sigma^+ + \mathrm{H.c.}] + \ldots. \quad (3)$$

Note how the pulse-to-pulse phase difference $\Delta\phi$ decreases the amplitude of the Rabi oscillations and can be measured. However, as we show later on, the functional dependence on $\Delta\phi$ implies a low sensitivity on the phase in practical implementations of the protocol.

We can do much better by changing the intensity regime to $\theta = \pi$ (protocol 1B), where each comb pulse can flip the state of the atom. Under these conditions, for an even set of pulses we get

$$U_{\mathrm{tot}}^{(1B)} = \prod_i U_i = \exp\left[-2i\sum_{k=1}^{N/2}(\phi_{2k} - \phi_{2k-1})\sigma^z\right], \quad (4)$$

which for constant $\Delta\phi$ implies $U_{\mathrm{tot}}^{(1B)} = \exp(-iN\Delta\phi\sigma^z)$. Now $\Delta\phi$ can be interferometrically detected with an enhancement proportional to the number of pulses N.

It is obvious that the sensitivity (4) increases by maximizing the phase difference between consecutive pulses. To profit from this, we design a set of protocols that extract a sequence of $N/2$ pulses from the original pulse train, and delay them a time $T_d \gg T$. This sequence is then intercalated with the original one, cf. Fig. 2(b), so that $\phi_{2k} = k\Delta\phi + \Delta\phi T_d/T$ and $\phi_{2k-1} = k\Delta\phi$. Introducing this sequence in Eqs. (3) and (4) we obtain, respectively, the unitaries corresponding to protocols 2A (for $\theta \ll 1$) and 2B ($\theta \sim \pi$). In particular, the unitary corresponding to protocol 2B is

$$U_{\mathrm{tot}}^{(2B)} = \exp(-i\sigma^z\Delta\phi \times NT_d/T), \quad (5)$$

with an additional enhancement factor $N_d = T_d/T$. This is optimal with respect to any rearrangement of the pulses, using each pulse only once.

Interferometry and sensitivity.—We now transfer the information of the acquired phase to the measurable populations of the atomic states. For this, we complete the previous unitaries with additional operations and measurements that enable estimating $\Delta\phi$ and θ. Out of $2M$ atoms, M are subject to the following steps [cf. Fig. 2(c)]: (i) initialization to the ground state $|0\rangle$, (ii) applying a $\pi/2$ rotation (which could be either $\exp(i\sigma_x\pi/4)$ or a Hadamard gate) onto the ground state, (iii) applying a reference phase ξ onto the level $|1\rangle$, (iv) letting the atom interact with the comb as described before, (v) undoing the $\pi/2$ rotation of step (i) and measuring the state of the atom, $s \in \{0, 1\}$. The measurement outcome is described by the probability distribution $P_1(s|\theta, \Delta\phi)$. For the remaining M atoms we skip (ii), obtaining the distribution $P_2(s|\theta, \Delta\phi)$. We remark that we need no phase coherence between the comb and the lasers that implement the $\pi/2$ rotations. The reference phase ξ is computed *a priori* to maximize the sensitivity of $P_{1,2}$ to the $\Delta\phi$.

The functions P_1 and P_2 convey all the information accessible in the lab: from the measurements of s in P_1 and P_2 experiments, one should compute different estimators and use them to infer the values of θ and $\Delta\phi$, with uncertainties σ_θ and $\sigma_{\Delta\phi}$. Using error propagation and the Fisher information we obtain fundamental lower bounds and practical estimates (see the Supplemental Material [36]) of the sensitivities ($\sigma_{\Delta\phi}^{-1}$ and σ_θ^{-1}) of each protocol. As summarized in Table I, it is possible to build estimators of minimal variance for θ and $\Delta\phi$, which saturate the fundamental lower bounds. Moreover, we observe that all protocols but 1A improve over the standard statistical sensitivity $\sqrt{M}$ thanks to the large number of pulses or to the use of pulses from well-separated times. In practice, both N and N_d span several orders of magnitude, providing a sensitivity comparable to the state of the art.

Three-level schemes.—In real atoms, if the qubit states 0 and 1 are dipole coupled by a comb, spontaneous emission may severely limit the total interrogation time. One solution is to use dipole-forbidden transitions restricted in practice to the $\theta \ll 1$ regime. An attractive alternative is the Λ scheme in Fig. 3, where two long-lived states $|0, 1\rangle$ talk via an intermediate level $|e\rangle$. Applying combs or other lasers with orthogonal polarizations on the legs of the Λ scheme, we can create effective Rabi oscillations between $|0\rangle$ and $|1\rangle$ while keeping a small population in $|e\rangle$ so that spontaneous emission is negligible.

A simple way to minimize spontaneous emission is to turn the Λ into a Raman scheme, detuning the lasers that couple $|0, 1\rangle$ with $|e\rangle$. Such Raman processes mix well with our algorithms. To start, if we have already stabilized the phase of a cw laser, we can combine it with the pulses from the comb [cf. Fig. 3(a)]. This process enables an accurate determination of the CEP with respect to the cw source. The result is a sequence of effective unitaries with an average Rabi angle θ' and a pulse phase $\phi'_m = \phi_m - \phi_{\text{ref}}$, where ϕ_{ref} is the phase of the stabilized source. The identifications $\theta \to \theta'$ and $\phi_m \to \phi'_m$ directly translate all protocols above to this new setup. Likewise, one may combine the FC with a stabilized one [cf. Fig. 3(b)] and use our protocols to reconcile them.

A more interesting use of Raman transitions is to achieve self-referencing of the comb. For this, we use the scheme from Fig. 3(b), combining two pulses from the same comb, but with a relative delay T_d, as in Fig. 2(b). This amounts to a self-referenced interferometric scheme based on time shifts, not requiring frequency shifting or shearing [23]. The phases of both pulses effectively combine in a nontrivial way in the unitary associated to the Raman process, $\phi'_m = \phi_m - \phi_{m-N_d} = N_d\Delta\phi$ (see the Supplemental Material [36]). We can apply a sequence of N pulse pairs with an effective angle θ' that should optimally lie around $N\theta' \simeq \pi/2$

$$U^{(1\text{A,Raman})} = e^{-iN_d\Delta\phi\sigma_z} e^{iN\frac{\theta'}{2}\sigma_x} e^{iN_d\Delta\phi\sigma_z} \tag{6}$$

and use Ramsey interferometry to measure both θ' and $\Delta\phi$. A generalization of protocols 2A and 2B is also possible using a linear optics circuit with two delay lines, so that each atom is hit by pairs of pulses with alternating phases $(\phi_m, \phi_{m-N_{d1}})$ and $(\phi_m, \phi_{m-N_{d2}})$. This leads to the sensitivities shown in the lower half of Table I.

Note that using Raman schemes demands the setup to be interferometrically stable up to a fraction of a wavelength.

TABLE I. Sensitivities $\sigma_{\Delta\phi,\theta}^{-1}$ of a set of $2M$ two- or three-level atoms to the protocols described in the text (1A, 1B, 2A, 2B). N is the number of pulses in a sequence, which in the delayed cases are combined with N pulses from a later time $T_d = N_dT$.

Implementation	$\theta \ll 1$ (A)	$\theta \simeq \pi$ (B)
Two levels, no delay (1)	$\sqrt{M}$	$N\sqrt{M}$
Two levels, with delay (2)	$N_d\sqrt{M}$	$NN_d\sqrt{M}$
Raman, one-delay (1)	$N_d\sqrt{M}$	...
Raman, two-delays (2)	$\lvert N_{d2} - N_{d1}\rvert\sqrt{M}$	$N\lvert N_{d2} - N_{d1}\rvert\sqrt{M}$

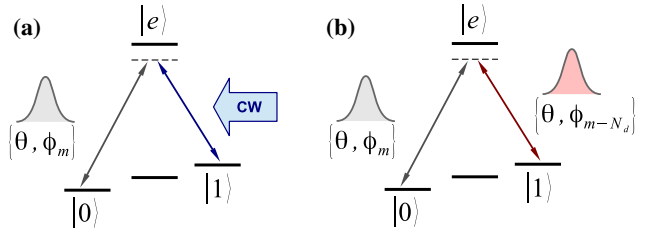

FIG. 3 (color online). The mth comb pulse interacts in a Raman setup with either (a) a cw laser signal or (b) another comb pulse. Controlling the polarization of the light and using the selection rules in atomic transitions we can ensure that each pulse or laser activates only one leg of the Λ scheme.

When a single pulse interacts with a two-level atom it does not matter whether the delay is a multiple of the comb period, or fails by a small amount, $\delta T = T_d - N_d T$ ($|\delta T| < T$). This is so because only the CEP enters the unitary and this only contains information on $\nu_0 N_d T$. However, in Raman schemes, where two pulses overlap in time, their relative delay is a new parameter that influences the effective Rabi angle as well as the phase. In particular, the phase difference reads (see the Supplemental Material [36]) $\Delta\phi' = \Delta\phi + \omega\delta T$, with a contribution due to the interferometric path $c\delta T$, which must be separately stabilized.

To remove the need for interferometric stability, we can use a different approach in which the comb only interacts with one transition, $|1\rangle \to |e\rangle$, performing π rotations, while $|0\rangle$ is a dark state. The unperturbed and delayed pulses arrive closely in pairs, but without temporal overlap, implementing the sequence $|1\rangle \to -e^{i(\phi_m - \phi_{m-N_d})}|1\rangle$. Due to the lack of overlap, the delay errors drop and the effective operation is a phase gate in the qubit space. Spontaneous emission lowers the visibility and it is small because $|e\rangle$ is populated only for a time $T_e = \mathcal{O}(\tau)$. Denoting by γ the spontaneous decay rate of $|e\rangle$, we may afford $N = -\log(\epsilon)/\gamma T_e$ pulses before the visibility decreases by ϵ. For a typical value $1/\gamma = 8$ ns and a safe $T_e = 100$ ps, visibility decreases just 10% for 200 pulses, sufficient to implement the last protocol in Table I.

Errors.—We can also account for ac Stark and Zeeman shifts in experiments. In both cases, the effect can be modeled (see the Supplemental Material [36]) as a random term in the Hamiltonian $\epsilon(t)\sigma_z$ that makes the atomic levels fluctuate on time scales much longer than τ. This induces an uncertainty in $\Delta\phi$ of order $\sigma_\epsilon \times (t_{m+1} - t_m)$, where σ_ϵ is the standard deviation of $\epsilon(t)$ from its (zero) average, and t_m is the arrival time of each pulse. This error is cancelled using spin-echo techniques [37] or, more directly, in protocols 2A and 2B, by calibrating the delays so that consecutive pulses arrive closely spaced but without overlap, say 10 ps apart. A pessimistic ac Stark shift $\sigma_\epsilon \sim 100$ Hz then induces an error $\leq 10^{-9}$ rad in $\Delta\phi$.

Another source of error is temperature: when atoms move between pulses, they sample the laser's spatial variations of phase and intensity. We can eliminate such errors (see the Supplemental Material [36]) by (i) working in a Raman configuration which transfers no net momentum to the atom and (ii) ensuring the lasers are not tightly focused. These techniques allow working with sympathetically Doppler cooled ions in fast experiments ($\sim 1 - 10$ ms from ion reset to detection).

The protocols discussed admit many implementations. For concreteness, we discuss here a setup with trapped ions, because of recent progress in connection with ultrafast lasers [38,39]. The long coherence times of ions, $t_{\mathrm{coh}} \sim 1$ s [40], allow us to consider trains of up to $t_{\mathrm{coh}}/T \sim 10^8$ pulses from a typical comb with $f_{\mathrm{rep}} \sim 100$ MHz [41]. In the Raman schemes, with one ion and one delay line, this allows us to detect CEP fluctuations $\delta\Delta\phi \sim 10^{-8}$ rad and calibrate the comb offset below $\delta\Delta\phi/T \sim 1$ Hz, a remarkable precision for 1 s of interrogation time. The numbers improve with a two-delay Raman scheme, reaching $\delta\Delta\phi \sim 10^{-15}$ where error sources become relevant. Precision decreases marginally, $\delta\Delta\phi \sim 10^{-5} - 10^{-10}$, using faster duty cycles with $\sim$1 ms of interrogation time (see the Supplemental Material [36]).

Applications.—In practical applications, the phase differences will be large. To avoid it wrapping around 2π, the number of pulses must be dynamically adjusted so that $N < 1/\Delta\phi$, increasing it only as the comb is better stabilized. Thus, measurement times cannot be longer than the typical time for the random fluctuations in ν_0. The precision limit is in practice set by the time scale at which we can provide useful feedback to the comb and not by the interferometric protocol.

We identify two frequency ranges where our protocol appears particularly useful. First, due to the technological and scientific interests of midinfrared ($\lambda = 2.5$–25 μm) FCs [42], we propose to use Ba^+ ions (that feature several narrow transitions around 2 μm) to stabilize a visible or near-IR FC at $\Delta\phi = 0$ so that difference-frequency generation from two of its teeth can produce a stabilized mid-IR FC. Secondly, Mg^+ presents various transitions around 280 nm which could be used to stabilize FCs in the near UV, with application in high-harmonic generation and strong-field physics. We discuss in the Supplemental Material [36] further details on current FC technologies, possible atom or ion stabilization systems, and a comparison between typical drift rates of an unlocked comb's frequency offset and the time scale of the atomic experiment.

Summing up, we presented several quantum inteferometric algorithms based on the idea that one atom may accumulate the effect of multiple laser pulses, computing their differences through the appropriate pulse ordering, intermediate gates, and measurements. MPQI protocols provide a polynomial sensitivity enhancement with respect to conventional atom or Ramsey interferometry. MPQI can be used to detect temporal changes in the CEP of a FC because the unitary implemented by a single pulse is sensitive to both the intensity and the CEP, and not to the pulse arrival time. The schemes presented are particularly suitable for nonoctave spanning combs with a low intrinsic phase noise, such as high-power Ti:sapphire lasers where significant phase noise is introduced by amplification stages. Our protocols can be generalized beyond the RWA and to characterize other properties of the comb, such as intensity fluctuations. We anticipate MPQI will enable new progress in fields as diverse as ultrafast science, frequency metrology, and direct frequency-comb spectroscopy, or coherent control of molecular processes.

We acknowledge very long and fruitful discussions with Piet O. Schmidt. This work has been funded by Spanish

MINECO Project FIS2012-33022, CAM research consortium QUITEMAD (S2009-ESP-1594), COST Action IOTA (MP1001), a Marie Curie Intra-European Fellowship, and the JAE-Doc program (CSIC).

[1] S. Haroche and D. J. Wineland, Nobel Prize in Physics in 2012. The prize was awarded jointly "for ground-breaking experimental methods that enable measuring and manipulation of individual quantum systems".
[2] D. Leibfried, R. Blatt, C. Monroe, and D. Wineland, Rev. Mod. Phys. **75**, 281 (2003).
[3] H. Häffner, C. Roos, and R. Blatt, Phys. Rep. **469**, 155 (2008).
[4] K. R. Brown, A. C. Wilson, Y. Colombe, C. Ospelkaus, A. M. Meier, E. Knill, D. Leibfried, and D. J. Wineland, Phys. Rev. A **84**, 030303 (2011).
[5] J. Benhelm, G. Kirchmair, C. F. Roos, and R. Blatt, Nat. Phys. **4**, 463 (2008).
[6] A. H. Myerson, D. J. Szwer, S. C. Webster, D. T. C. Allcock, M. J. Curtis, G. Imreh, J. A. Sherman, D. N. Stacey, A. M. Steane, and D. M. Lucas, Phys. Rev. Lett. **100**, 200502 (2008);
[7] A. H. Burrell, D. J. Szwer, S. C. Webster, and D. M. Lucas, Phys. Rev. A **81**, 040302(R) (2010).
[8] S. Olmschenk, R. Chicireanu, K. D. Nelson, and J. V. Porto, New J. Phys. **12**, 113007 (2010).
[9] A. Widera, O. Mandel, M. Greiner, S. Kreim, T. W. Hänsch, and I. Bloch, Phys. Rev. Lett. **92**, 160406 (2004).
[10] J. Mur-Petit, J. J. Garcia-Ripoll, J. Pérez-Ríos, J. Campos-Martínez, M. I. Hernández, and S. Willitsch, Phys. Rev. A **85**, 022308 (2012).
[11] D. Leibfried, New J. Phys. **14**, 023029 (2012).
[12] S. Ding and D. N. Matsukevich, New J. Phys. **14**, 023028 (2012).
[13] P. O. Schmidt, T. Rosenband, C. Langer, W. M. Itano, J. C. Bergquist, and D. J. Wineland, Science **309**, 749 (2005).
[14] C. W. Chou, D. B. Hume, J. C. J. Koelemeij, D. J. Wineland, and T. Rosenband, Phys. Rev. Lett. **104**, 070802 (2010).
[15] W. Wasilewski, K. Jensen, H. Krauter, J. J. Renema, M. V. Balabas, and E. S. Polzik, Phys. Rev. Lett. **104**, 133601 (2010).
[16] M. Napolitano, M. Koschorreck, B. Dubost, N. Behbood, R. J. Sewell, and M. W. Mitchell, Nature (London) **471**, 486 (2011).
[17] P. K. Jha, Y. V. Rostovtsev, H. Li, V. A. Sautenkov, and M. O. Scully, Phys. Rev. A **83**, 033404 (2011).
[18] G. Paulus, F. Grasbon, H. Walther, P. Villoresi, M. Nisoli, S. Stagira, E. Priori, S. De Silvestri, Nature (London) **414**, 182 (2001).
[19] A. Baltuška, T. Udem, M. Uiberacker, M. Hentschel, E. Goulielmakis, C. Gohle, R. Holzwarth, V. S. Yakovlev, A. Scrinzi, T. W. Hänsch, and F. Krausz, Nature (London) **421**, 611 (2003).
[20] T. M. Fortier, P. A. Roos, D. J. Jones, S. T. Cundiff, R. D. R. Bhat, and J. E. Sipe, Phys. Rev. Lett. **92**, 147403 (2004).
[21] P. Roos, X. Li, R. Smith, J. A. Pipis, T. Fortier, and S. T. Cundiff, Opt. Lett. **30**, 735 (2005).
[22] T. Wittmann, B. Horvath, W. Helml, M. G. Schätzel, X. Gu, A. L. Cavalieri, G. Paulus, and R. Kienberger, Nat. Phys. **5**, 357 (2009).
[23] I. A. Walmsley and C. Dorrer, Adv. Opt. Photonics **1**, 308 (2009).
[24] L. Xu, C. Spielmann, A. Poppe, T. Brabec, F. Krausz, and T. Hänsch, Opt. Lett. **21**, 2008 (1996).
[25] K. Osvay, M. Görbe, C. Grebing, and G. Steinmeyer, Opt. Lett. **32**, 3095 (2007).
[26] T. Udem, R. Holzwarth, and T. W. Hänsch, Nature (London) **416**, 233 (2002).
[27] J. Ye and S. T. Cundiff, *Femtosecond Optical Frequency Comb: Principle, Operation, and Applications* (Springer-Verlag, Berlin, 2005).
[28] J. Reichert, R. Holzwarth, T. Udem, and T. Hänsch, Opt. Commun. **172**, 59 (1999).
[29] D. J. Jones, S. A. Diddams, J. K. Ranka, A. Stentz, R. S. Windeler, J. L. Hall, and S. T. Cundiff, Science **288**, 635 (2000).
[30] A. Marian, M. C. Stowe, J. R. Lawall, D. Felinto, and J. Ye, Science **306**, 2063 (2004).
[31] S. Witte, R. T. Zinkstok, W. Ubachs, W. Hogervorst, and K. S. E. Eikema, Science **307**, 400 (2005).
[32] A. L. Wolf, S. A. van den Berg, W. Ubachs, and K. S. E. Eikema, Phys. Rev. Lett. **102**, 223901 (2009).
[33] A. L. Wolf, J. Morgenweg, J. C. J. Koelemeij, S. A. van den Berg, W. Ubachs, and K. S. E. Eikema, Opt. Lett. **36**, 49 (2011).
[34] D. Felinto and C. E. E. López, Phys. Rev. A **80**, 013419 (2009).
[35] We can develop the MPQI protocols using the numerical expressions of the unitary operators when the RWA does not apply.
[36] See Supplemental Material at http://link.aps.org/supplemental/10.1103/PhysRevLett.112.073603 for full details of the approximations and numerical calculations, including modelling of experimental errors and practical implementations.
[37] N. Kurnit, I. Abella, and S. Hartmann, Phys. Rev. Lett. **13**, 567 (1964).
[38] W. C. Campbell, J. Mizrahi, Q. Quraishi, C. Senko, D. Hayes, D. Hucul, D. N. Matsukevich, P. Maunz, and C. Monroe, Phys. Rev. Lett. **105**, 090502 (2010).
[39] J. Mizrahi, C. Senko, B. Neyenhuis, K. G. Johnson, W. C. Campbell, C. W. S. Conover, and C. Monroe, Phys. Rev. Lett. **110**, 203001 (2013).
[40] S. Olmschenk, K. C. Younge, D. L. Moehring, D. N. Matsukevich, P. Maunz, and C. Monroe, Phys. Rev. A **76**, 052314 (2007).
[41] We discuss the maximum number of phase-coherent consecutive pulses in Ref. [36].
[42] A. Schliesser, N. Picqué, and T. W. Hänsch, Nat. Photonics **6**, 440 (2012).